



Structural and functional characterization of simvastatin-induced myotoxicity in different skeletal muscles

Nihal Simsek Ozek^{a,b}, I. Burak Bal^c, Yildirim Sara^c, Rustu Onur^c, Feride Severcan^{a,*}

^a Department of Biological Sciences, Middle East Technical University, 06800 Ankara, Turkey

^b Department of Biology, Ataturk University, 25240 Erzurum, Turkey

^c Department of Pharmacology, Faculty of Medicine, Hacettepe University, 06100 Ankara, Turkey

ARTICLE INFO

Article history:

Received 22 February 2013

Received in revised form 20 July 2013

Accepted 6 September 2013

Available online 15 September 2013

Keywords:

Statin

Extensor digitorum longus

Soleus

Diaphragm

Contractility

Fourier Transform Infrared spectroscopy

ABSTRACT

Background: Statins are the most commonly used drugs for the treatment of hypercholesterolemia. Their most frequent side effect is myotoxicity. To date, it remains unclear whether statins preferentially induce myotoxicity in fast- or in slow-twitch muscles. Therefore, we investigated these effects on fast- (extensor digitorum longus; EDL), slow- (soleus; SOL), and mixed-twitch muscles (diaphragm; DIA) in rats by comparing their contractile and molecular structural properties.

Methods: Simvastatin-induced functional changes were determined by muscle contraction measurements, and drug-induced molecular changes were investigated using Fourier transform infrared (FTIR) and attenuated total reflectance (ATR) FTIR spectroscopy.

Results: With simvastatin administration (30 days, 50 mg/kg), a depression in the force–frequency curves in all muscles was observed, indicating the impairment of muscle contractility; however, the EDL and DIA muscles were affected more severely than the SOL muscle. Spectroscopic findings also showed a decrease in protein, glycogen, nucleic acid, lipid content and an increase in lipid order and lipid dynamics in the simvastatin-treated muscles. The lipid order and dynamics directly affect membrane thickness. Therefore, the kinetics and functions of membrane ion channels were also affected, contributing to the statin-induced impairment of muscle contractility. Furthermore, a reduction in α -helix and β -sheet and an increase in random coil, aggregated and antiparallel β -sheet were observed, indicating the protein denaturation. Spectral studies showed that the extent of molecular structural alterations in the muscles following simvastatin administration was in the order EDL > DIA > SOL.

Conclusions: Simvastatin-induced structural and functional alterations are more profound in the fast-twitch than in the slow-twitch muscles.

General significance: Myotoxic effects of simvastatin are primarily observed in the fast-twitch muscles.

© 2013 Elsevier B.V. All rights reserved.

1. Introduction

Statins, which are selective 3-hydroxy-3-methylglutaryl-coenzyme A (HMG-CoA) reductase inhibitors, reduce morbidity and mortality in patients with coronary artery and cerebrovascular diseases [1]. Although they are generally well tolerated, they sometimes have adverse effects, mainly related to skeletal muscles. These side effects vary depending on the lipophilic properties of statins [2–4]. Lipophilic statins enter the cell by simple diffusion, and their toxic effects on nonhepatic tissues are greater than those of hydrophilic statins [5]. Muscular side effects

range from mild myopathy, characterized by fatigue, weakness, and serum creatine kinase elevation, to rhabdomyolysis [1].

Previous studies on statin-induced myotoxicity have suggested that statins decrease the membrane cholesterol content in myocytes, which may alter the cell membrane fluidity and contractile function and T-tubular system structure of muscle cells [6,7]. It was reported that statins reduce chloride conductance, which leads to myotoxic symptoms in rats [8]. Another possible mechanism is through a statin-related impairment of the mevalonate pathway caused by decreasing heme A, ubiquinone levels, and protein prenylation. Decreased heme A and ubiquinone levels are also reported to impair energy metabolism in skeletal muscles by disrupting mitochondrial electron transport mechanisms [9]. In addition, statins were shown to cause apoptosis of muscle cells by downregulating protein prenylation [10].

Although several studies have been conducted to elucidate the myotoxic effects of statins on the biochemical and genetic levels, the structural and functional alterations induced by statins in skeletal muscle macromolecules have not yet been clarified. In a previous study examining these alterations, we investigated the effects of low-dose

Abbreviations: FTIR, Fourier transform infrared spectroscopy; ATR-FTIR, attenuated total reflectance Fourier transform infrared spectroscopy; EDL, extensor digitorum longus; DIA, diaphragm; SOL, soleus

* Corresponding author at: Department of Biological Sciences, Middle East Technical University, Dumlupinar Blv. No: 1, 06800 Ankara, Turkey. Tel.: +90 312 210 5166; fax: +90 312 210 79 76.

E-mail addresses: ozek@metu.edu.tr (N. Simsek Ozek), burakbal@gmail.com (I.B. Bal), ysara@hacettepe.edu.tr (Y. Sara), ronur@hacettepe.edu.tr (R. Onur), feride@metu.edu.tr (F. Severcan).

simvastatin on EDL muscle. A reduction in the protein, nucleic acid, and saturated and unsaturated lipid contents and an increase in the membrane fluidity and lipid order were found in simvastatin-treated EDL muscle [11].

Several studies on the fiber selectiveness of statin myotoxicity revealed that the myotoxic effects of statins are different in different skeletal muscles depending on their fiber-type structure. For example, histopathological examinations done by Westwood et al. indicated that slow-twitch (type-I) fibers were not affected by statin-induced muscle necrosis [12]. However, another recent study showed that type-I fibers were predominantly affected by cerivastatin-induced myotoxicity [13]. Thus, whether the statins primarily affect fast- or slow-twitch muscles is still unclear. Therefore, the purpose of the current study was to determine the preferential target muscle for statin-induced myotoxicity by comparing the differential effects of chronic simvastatin treatment on three different rat skeletal muscles, namely, fast- (EDL), slow- (SOL), and mixed-twitch (DIA) muscles, based on the evaluation of their contractile and structural properties. Simvastatin-induced molecular changes were investigated using Fourier transform infrared (FTIR) and attenuated total reflectance (ATR) FTIR spectroscopy. Infrared spectroscopy is a powerful analytical technique based on the absorption of infrared photons that excite vibrations of molecular bonds. Because IR data are stored in digitally encoded formats, spectral data can be easily interpreted and small changes can be accurately detected, even in the weak absorption bands, using post-acquisition data manipulation algorithms [14]. Therefore, FTIR spectroscopy is commonly used in a number of branches of science as a quantitative and qualitative tool. It is a fast, nondestructive technique (needs no probe) that provides rapid, sensitive, and simultaneous monitoring of the different macromolecular functional groups in biological systems without requiring large sample quantities. Therefore, it has emerged as an ideal tool that gives valuable information about the changes in biochemical components and processes in diseases or drug-induced pathological conditions [11,15].

2. Materials and methods

2.1. Chemicals

Simvastatin was purchased from Merck, Sharp and Dohme (West Point, PA, USA) and dissolved in saline. Butylated hydroxytoluene, cholesterol, and caffeine were obtained from Sigma Chemical Company (Saint Louis, MO, USA). Potassium bromide (KBr), acetonitrile, and methanol were obtained from Merck (Darmstadt, Germany).

2.2. Animals

Experiments were performed on male Wistar rats (12–14 weeks) weighing 250–300 g. The study was approved by the Animal Ethical Committee of Hacettepe University. The rats were fed a standard diet with water ad libitum and kept in a room with controlled light cycles (12:12 h, dark:light), temperature ($22 \pm 1^\circ\text{C}$), and relative humidity (40–50%). They were allowed to adapt to their environment for 1 week prior to the experiments. Rats were randomly allocated into two groups (eight in each group) to receive either simvastatin or saline. Simvastatin (50 mg/kg in saline) was administered through oral gavage for 30 days. The 50 (mg/kg)/day dose of the simvastatin was chosen according to a previous animal study [16]. During the experiment period, the rats were weighed weekly, and their food and water consumption was measured daily.

At the end of the treatment period, rats were anesthetized with diethyl ether, and blood samples were drawn. The muscles were dissected, and one of each muscle pair was frozen (-80°C) for the FTIR studies. Contractility studies were performed on the other pairs.

2.3. Contractility studies

The muscles were kept in Krebs's solution (composition in mM: 135 NaCl, 5 KCl, 1 MgCl_2 , 2 CaCl_2 , 15 NaHCO_3 , 1 Na_2HPO_4 , 11 glucose). Solutions were maintained at $37 \pm 0.5^\circ\text{C}$ and pH ~ 7.4 by gassing with 5% CO_2 and 95% O_2 .

The muscles were isolated and bathed in organ baths. The contractile properties of the EDL and SOL were studied in the whole muscle preparations, whereas the contractile properties of DIA muscle were performed on muscle strips of $\sim 5 \times 17$ mm. Contractile force was measured by FT-03 force transducers connected to a polygraph (7B Grass Instruments, Quincy, MA, USA). A holder attached to a micrometer allowed us to adjust the optimal tension, which was defined as the tension at which the twitch amplitude was maximum. Optimal tensions were ~ 2 g and were kept constant throughout the experiments. Following a 1 h equilibration period, isometric contractions were evoked by field stimulation with pulses of 1 ms in duration and 150 V. For all stimulations, S88 Grass stimulators and stimulus isolation units (Grass SIU 5) were used.

The tetanic force–frequency relationship was evaluated by applying trains of 500 ms in duration between 0.1 and 120 Hz every 3 min. Amplifier outputs were also fed to a data acquisition unit (Powerlab/8SP, ADInstruments, Australia), and the force expressed in Newtons was normalized by the muscle cross-sectional area. Nonmuscle tissue was removed, the muscles were blotted and weighed, and forces per cross-sectional area were calculated according to the following equation: $\text{force}/\text{cm}^2 = [\text{force (N)} \times \text{specific density of skeletal muscle (1.06 g}/\text{cm}^3) \times \text{length of muscle (cm)}] / [\text{mass of muscle (g)}]$. To induce contractions via caffeine, the solution was changed to one containing 20 mM caffeine.

2.4. Determination of total serum cholesterol, total serum creatine kinase (CK) activity, and myoglobin content

The total cholesterol level was determined by HPLC as described in [17]. The serum total CK activity and myoglobin content were determined by a Roche Cobas Integra 800 analyzer and Roche Diagnostic kits (Roche Diagnostics, GmbH, Mannheim, Germany).

2.5. FTIR and ATR-FTIR studies

For the FTIR studies, the freeze-dried (Labconco FreeZone®, Freeze Dry System Model 77520, USA) EDL and SOL samples were ground in a liquid-nitrogen-cooled colloid mill (Retsch MM200, GmbH, Germany) and then mixed with dried KBr in a mortar (at a ratio of 0.5:150). After drying again in the freeze drier for 18 h to remove unbound or free water, the mixture was compressed into a thin KBr disk under a pressure of ~ 100 kg/cm², producing a transparent disk for the FTIR measurements.

Infrared spectra of the EDL and SOL samples were obtained using a PerkinElmer Spectrum 100 FTIR spectrometer (PerkinElmer Inc., Norwalk, CT, USA) equipped with a mid-infrared (MIR) tryglycine sulfate (TGS) detector. The interfering spectra from air and the KBr transparent disk were recorded as background and subtracted automatically using the appropriate software (Spectrum 100 software). The spectra of muscle samples were recorded in the 4000–400 cm^{-1} region at room temperature. A total of 50 scans was taken for each interferogram at 4 cm^{-1} resolution.

Due to the problems in grinding the dried DIA muscles, we examined this muscle directly using ATR-FTIR spectroscopy. For the ATR-FTIR studies, samples $0.5 \times 0.5 \times 0.1$ cm in size were cut from rat DIA. They were then directly placed on the ATR crystal and compressed (150 gauge) to obtain good surface contact.

The infrared spectra of the DIA samples were collected in the one-bounce ATR mode on a Spectrum 100 FTIR spectrometer equipped with a universal ATR accessory. The diaphragm muscle samples were placed on a diamond/ZnSe crystal plate, and 50 scans with a resolution

of 4 cm^{-1} were collected at room temperature in the region from 4000 to 650 cm^{-1} . Water was used as a reference and was subtracted automatically from the tissue spectra.

The spectra collection and data manipulation were carried out using Spectrum 100 software (PerkinElmer). Each sample was scanned in triplicate under the same conditions, giving identical spectra. The average spectra of these replicates were used in the subsequent detailed data and statistical analyses. The spectra were first smoothed with a nine-point Savitzky–Golay smoothing function to remove the noise. The average spectra were baseline corrected and normalized with respect to the specific bands for visual demonstration. The band positions were measured using the frequency corresponding to the center of weight. Band areas were calculated from the smoothed and baseline-corrected spectra using the Spectrum software. The bandwidth values of specific bands were calculated as the width of $0.75 \times$ height of the signal in units of cm^{-1} .

The amide I band was used to determine the simvastatin-induced variations in protein secondary structure, and a detailed analysis was carried out using the OPUS^{NT} data collection software. The second derivatives of the spectra were vector normalized at $1700\text{--}1600\text{ cm}^{-1}$, and the intensities of peaks were calculated. Because the peak positions of the original absorption spectra correspond to the minimum positions in the second derivative spectra, the minimum positions were used for comparisons.

2.6. Cluster analysis

Hierarchical cluster analysis (HCA) was performed by using OPUS 5.5 software (Bruker Optics, GmbH, Germany) to differentiate and characterize the skeletal muscles based on spectral variations. The second derivative of each spectrum was taken in the $3050\text{--}1000\text{ cm}^{-1}$ region. Spectral distances were calculated between pairs of spectra as Pearson's correlation coefficients. The cluster analysis for the separation of control and treatment groups was based on the Euclidean distances. Ward's algorithm was used to construct dendrograms.

2.7. Statistical analysis

All data were expressed as mean \pm SEM. The data obtained from the contractile experiments were tested for statistical significance using two-tailed, unpaired Student's *t*-tests. Spectroscopic results were tested for differences using the Mann–Whitney *U* test. *p* values < 0.05 were considered significant.

3. Results

3.1. Animals

Simvastatin-treated rats weighed significantly less following the treatment period (Table 1). The daily food and water intake of the simvastatin-treated animals was significantly lower than that of

the controls (Table 1). The simvastatin-treated rats also displayed a hunched posture, thin and pale appearance, body-weight loss, and decreased appetite during the last 10 days of statin administration.

3.2. Total serum cholesterol, total serum CK, and myoglobin

After 30 days, the serum cholesterol levels of the simvastatin-treated rats were significantly lower than that of control animals (Table 2). To test the myotoxicity of simvastatin, serum myoglobin content and serum total CK activity were measured. With simvastatin treatment, the CK activity significantly increased. Moreover, a significant rise in the serum myoglobin content of simvastatin-treated rats was found (Table 2).

3.3. Contractility measurements

The EDL, SOL, and DIA contractility measurements of simvastatin-treated and control animals revealed that simvastatin treatment did not appreciably alter the EDL and SOL skeletal muscle weights. In the control group, the EDL and SOL weighed $178 \pm 8.9\text{ mg}$ and $211.4 \pm 17\text{ mg}$, whereas the EDL and SOL were $187.0 \pm 7.6\text{ mg}$ and $189.5 \pm 15.8\text{ mg}$, respectively, in the simvastatin group. Because we used muscle strips instead of whole muscles, weight comparisons were not applicable for the DIA.

Twitch amplitudes were found to be significantly lowered by simvastatin treatment in the EDL muscles ($p < 0.05$), whereas amplitudes were unchanged in the SOL and DIA muscles. In the control and simvastatin groups, the twitch amplitudes were 2.6 ± 0.1 and 2 ± 0.1 for the EDL, 2.3 ± 0.3 and 2.2 ± 0.1 for the DIA, and 2.4 ± 0.4 and 2.3 ± 0.2 for the SOL muscles, respectively. The time courses of the twitches obtained from simvastatin-treated rat muscles were not different from that of their respective control muscles. To observe the effects of chronic simvastatin administration during intense muscle activity, we compared the force–frequency response curves within a stimulation range of $5\text{--}120\text{ Hz}$ (Fig. 1). A comparison of the force–frequency curves of the control and treatment groups showed a statistically significant depression of force production in all muscles studied ($p < 0.01$). This depression was greater at frequencies higher than 80 Hz in all muscles. Around a 30% reduction in the force production of the EDL and DIA was observed, whereas the SOL displayed a 22% inhibition of contractility following simvastatin treatment.

To evaluate the effects of simvastatin treatment on the further stages of excitation–contraction coupling, we used caffeine, which is a well-known inducer of Ca^{2+} release from the sarcoplasmic reticulum (SR). The introduction of 20 mM caffeine induced a slowly rising contraction. In the EDL and DIA muscles, chronic simvastatin-treatment significantly decreased the amplitude of caffeine-induced contractions without changing their time courses (Table 3). However, caffeine-induced contractions of the SOL muscles were not affected.

3.4. FTIR spectroscopy

Simvastatin-induced changes in macromolecular content, structure, and function were determined from a detailed analysis of the muscle

Table 1
Food intake, water intake, and body weight in rats treated with simvastatin.

	Control (n = 8)	Simvastatin-treated (n = 8)
Initial body weight (g)	262 ± 4.2	277 ± 3.9
Final body weight (g)	$267 \pm 5.3\uparrow$	$260 \pm 4.6\downarrow^*$
Food intake (g/rat)	19.1 ± 0.9	$15.5 \pm 1.0\downarrow^{**}$
Water intake (ml/rat)	29.8 ± 1.5	$21.2 \pm 1.1\downarrow^{***}$

Values are the mean \pm SEM for each group. Comparisons were done using Mann–Whitney *U* test. In body weight, downward arrow indicates a decrease and upward arrow indicates an increase with respect to the initial weight of each group. In food and water intake, downward arrow indicates a decrease and upward arrow indicates an increase with respect to the control.

* $p < 0.05$.

** $p < 0.01$.

*** $p < 0.001$.

Table 2
Total serum cholesterol level, total creatine kinase (CK) activity, and myoglobin content in control and simvastatin-treated animals.

	Control (n = 8)	Simvastatin-treated (n = 8)
Total cholesterol (mg/dl)	17.2 ± 1.2	$14.7 \pm 1.1\downarrow^{**}$
Total creatine kinase (U/l)	4550.38 ± 232.96	$11571.89 \pm 1336.02\uparrow^{***}$
Myoglobin (ng/ml)	81.17 ± 4.15	$137.06 \pm 8.94\uparrow^{***}$

Values are the mean \pm SEM for each group. Comparisons were made using Mann–Whitney *U* test. Downward arrow indicates a decrease and upward arrow indicates an increase with respect to the control.

** $p < 0.01$.

*** $p < 0.001$.

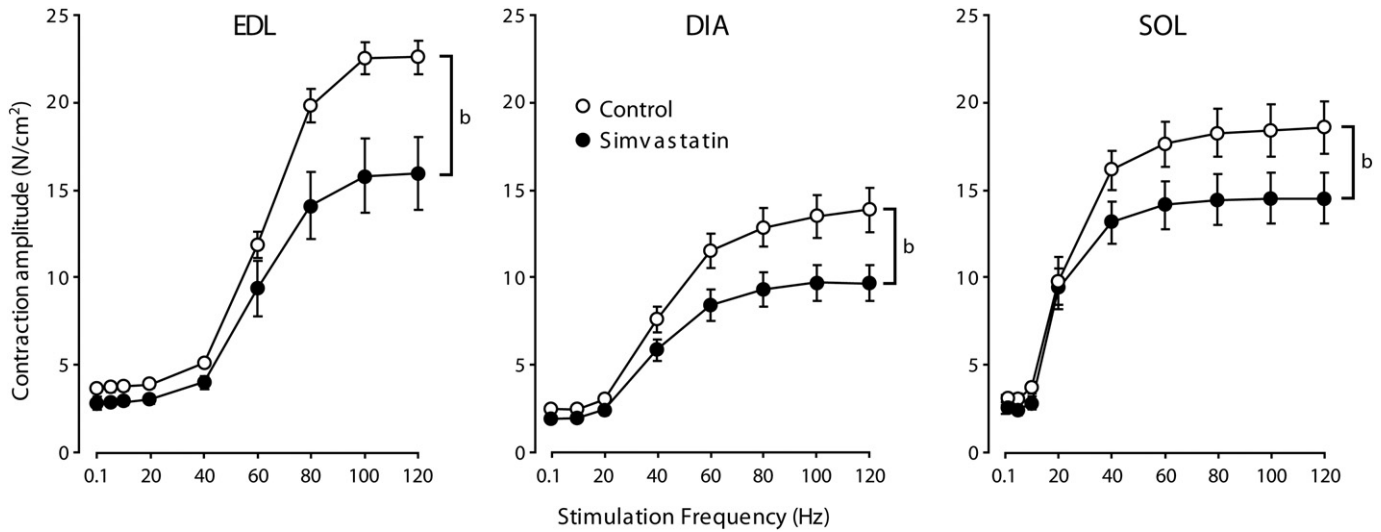


Fig. 1. Effects of chronic simvastatin treatment on contractility in rat extensor digitorum longus (EDL), diaphragm (DIA), and soleus (SOL) muscles. Twitches (0.1 Hz) and tetanic contractions (5–120 Hz) were induced by electrical field stimulation. Chronic simvastatin treatment depressed the force–frequency curves in all three muscles, affecting the EDL and DIA more severely than the SOL, for the same twitch amplitudes. Values are presented as mean \pm SEM.

spectra, and these values were compared for the first time for different skeletal muscles. The characteristic frequencies and detailed band assignments are given in Table 4 and Fig. 2. The alterations in the band area and frequency values together with the percent changes in the simvastatin-treated samples are compared in Table 5 with respect to the control group. The variations in the band positions of the CH_2 stretching bands (labeled as 2 and 4 in Fig. 2) give structural information, such as lipid order–disorder, whereas the signal intensity or, more accurately, the area under the bands reveals the concentration of the functional group belonging to the relevant molecule [11].

To investigate the effects of simvastatin treatment on the protein content of the skeletal muscles, the amide I and amide II bands (labeled as 6 and 7, respectively) were analyzed [11,15]. Although chronic simvastatin treatment reduced the protein content of the muscles studied, these reductions reached statistical significance in the EDL and DIA

muscles (Table 5). Simvastatin treatment also caused a significant shift in the frequencies of amide bands. The bandwidth values of the amide I band decreased in all treated groups but more dramatically for the EDL from 26.46 ± 0.34 to 25.43 ± 0.33 ($p < 0.05$). For the other muscles, no significant variations were observed.

Simvastatin-induced alterations in the protein secondary structure were determined from the intensity values of the second derivative sub-bands of the amide I band (Fig. 3, Table 6) [11,15]. Simvastatin treatment significantly decreased the intensities of the α -helical and β -sheet bands and increased the intensities of random coil, antiparallel β -sheet, and aggregated β -sheet bands of EDL muscle. The changes in the secondary structures for the DIA and SOL were not significant.

The effects of simvastatin treatment on saturated lipids were investigated by analyzing the CH_2 asymmetric stretching band (labeled as 2 in Fig. 2) [11]. Following simvastatin treatment, the band area of the

Table 3
Amplitudes and time course of caffeine-induced contractions in simvastatin-treated and control muscles.

Caffeine	Control (n = 8)			Simvastatin-treated (n = 8)		
	EDL	DIA	SOL	EDL	DIA	SOL
Peak amplitude (N/cm ²)	7.0 \pm 0.2	3.8 \pm 0.4	9.2 \pm 0.3	6.1 \pm 0.3*	3.0 \pm 0.1*	8.7 \pm 0.5
Time to peak (min)	38.3 \pm 2.2	3.8 \pm 0.1	20.5 \pm 2.4	34.5 \pm 1.8	3.5 \pm 0.2	20.0 \pm 4.2

Values are the mean \pm SEM for each group.

* $p < 0.05$.

Table 4
General band assignment of rat skeletal muscle [11,15].

Band no.	Wavenumber (cm ⁻¹)	Definition of the spectral assignment
1	3014	Olefinic=CH stretching vibration: unsaturated lipids and cholesterol esters
2	2929	CH_2 asymmetric stretching: mainly lipids, with little contribution from proteins, carbohydrates, and nucleic acids
3	2874	CH_3 symmetric stretching: mainly proteins, with little contribution from lipids, carbohydrates, and nucleic acids
4	2855	CH_2 symmetric stretching: mainly lipids, with little contribution from proteins, carbohydrates, and nucleic acids
5	1739–1744	Ester C=O stretch: triglycerides and cholesterol esters
6	1656	Amide I (protein, mainly C=O stretching)
7	1540	Amide II (protein, N–H bend, C–N stretch)
8	1343	CH_2 side chains of collagen
9	1261	PO_2^- asymmetric stretching, non-hydrogen bonded: mainly nucleic acids with the little contribution from phospholipids
10	1236	PO_2^- asymmetric stretching, fully hydrogen bonded: mainly nucleic acids with little contribution from phospholipids
11	1170	CO–O–C asymmetric stretching: ester bonds in cholesterol esters and phospholipids
12	1080	PO_2^- symmetric stretching: nucleic acids and phospholipids C–O stretch: glycogen, polysaccharides, and glycolipids
13	1040	C–O stretching: polysaccharides (glycogen)

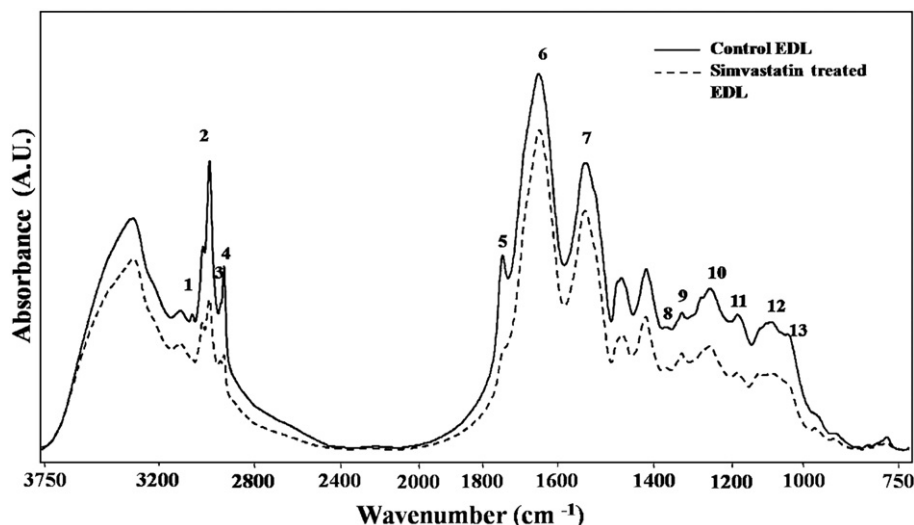


Fig. 2. Representative infrared spectra of control and simvastatin-treated EDL muscles in the 3750–750 cm^{-1} region.

EDL significantly decreased, and the frequency of the band shifted significantly to lower values (Table 5). The bandwidth of the CH_2 asymmetric stretching band also significantly increased in all muscles (EDL: from 11.34 ± 0.08 to 11.59 ± 0.03 , $p < 0.01$, DIA: from 10.30 ± 0.01 to 10.44 ± 0.03 , $p < 0.05$, SOL: from 11.78 ± 0.02 to 11.89 ± 0.03 , $p < 0.05$).

The lipid-to-protein ratio was derived from the ratio of the total area of the CH_2 asymmetric and symmetric stretching bands (bands 2 and 4) to the area of the CH_3 symmetric stretching band (band 3). Simvastatin treatment significantly increased the ratio of these bands in EDL muscle from 5.57 ± 0.02 to 6.80 ± 0.06 ($p < 0.05$).

The olefinic band was examined to investigate the unsaturated lipid content (band 1) [11,15]. A significant decrease in the area of this band was observed for the EDL and DIA but not the SOL muscles after simvastatin treatment.

The ratio of the total area of the CH_2 asymmetric and symmetric stretching bands (bands 2 and 4) to the area of the olefinic band (band 1) was calculated to examine simvastatin-induced changes in the saturated-to-unsaturated lipid ratio [11]. Simvastatin treatment led to a significant increase in this ratio in EDL muscle from 3.59 ± 0.13 to 5.05 ± 0.38 ($p < 0.01$), whereas the increase in the other muscle types did not reach statistical significance.

Table 5

Changes in the band area and frequency values of the infrared bands for control and simvastatin-treated, EDL, DIA, and SOL muscles.

Band no.	EDL			DIA			SOL		
	Control (n = 8)	Simvastatin (n = 8)	% change ^a	Control (n = 8)	Simvastatin (n = 8)	% change	Control (n = 8)	Simvastatin (n = 8)	% change
Band area									
1	1.26 ± 0.07	0.72 ± 0.05 ↓	−42.86	0.69 ± 0.01	0.62 ± 0.01 ↓	−10.14	0.93 ± 0.05	0.89 ± 0.03 ↓	−4.30
2	3.44 ± 0.07	3.08 ± 0.10 ↓	−10.47	2.90 ± 0.08	2.71 ± 0.03 ↓	−6.55	4.15 ± 0.22	3.98 ± 0.18 ↓	−4.10
3	0.99 ± 0.04	0.38 ± 0.04 ↓	−61.62	0.53 ± 0.01	0.49 ± 0.01 ↓	−7.55	0.49 ± 0.02	0.42 ± 0.01 ↓	−14.29
4	0.83 ± 0.04	0.45 ± 0.03 ↓	−45.78	0.61 ± 0.02	0.53 ± 0.01 ↓	−13.11	1.07 ± 0.09	0.96 ± 0.06 ↓	−10.28
5	3.68 ± 0.14	2.57 ± 0.10 ↓	−30.16	0.32 ± 0.02	0.31 ± 0.02 ↓	−3.13	3.38 ± 0.13	2.73 ± 0.12 ↓	−19.23
6	30.4 ± 1.72	18.90 ± 1.73 ↓	−37.83	20.63 ± 0.58	18.23 ± 0.45 ↓	−11.63	16.32 ± 0.94	14.68 ± 1.49 ↓	−10.05
7	11.79 ± 1.22	5.96 ± 0.55 ↓	−49.45	17.25 ± 0.29	15.94 ± 0.33 ↓	−7.59	11.26 ± 0.62	10.56 ± 0.86 ↓	−6.22
8	1.18 ± 0.05	0.99 ± 0.04 ↓	−16.10	2.58 ± 0.06	2.37 ± 0.06 ↓	−8.14	1.07 ± 0.04	1.01 ± 0.03 ↓	−5.61
9	1.77 ± 0.04	1.01 ± 0.05 ↓	−42.94	2.22 ± 0.04	1.96 ± 0.04 ↓	−11.71	1.21 ± 0.03	1.10 ± 0.03 ↓	−9.09
10	3.92 ± 0.17	3.03 ± 0.16 ↓	−22.70	5.93 ± 0.1	5.41 ± 0.1 ↓	−8.77	3.33 ± 0.09	3.15 ± 0.11 ↓	−5.41
11	1.88 ± 0.02	1.53 ± 0.03 ↓	−18.62	2.10 ± 0.04	2.07 ± 0.02 ↓	−1.43	3.17 ± 0.11	2.95 ± 0.08 ↓	−6.94
12	2.36 ± 0.07	1.85 ± 0.09 ↓	−21.61	4.94 ± 0.09	4.59 ± 0.04 ↓	−7.09	2.28 ± 0.02	2.17 ± 0.02 ↓	−4.82
13	1.92 ± 0.08	0.25 ± 0.09 ↓	−86.98	1.54 ± 0.03	1.38 ± 0.02 ↓	−10.39	1.94 ± 0.03	1.81 ± 0.03 ↓	−6.70
Band frequency									
2	2927.60 ± 0.21	2926.82 ± 0.22 ↓	−0.03	2927.71 ± 0.42	2927.39 ± 0.2 ↓	−0.01	2925.99 ± 0.09	2925.89 ± 0.07 ↓	−0.00
5	1742.94 ± 0.16	1746.41 ± 0.34 ↑	+0.20	1742.60 ± 0.59	1743.26 ± 0.50 ↑	+0.04	1744.28 ± 0.43	1745.34 ± 0.37 ↑	+0.06
6	1655.13 ± 0.18	1656.40 ± 0.21 ↑	+0.08	1636.32 ± 0.41	1637.26 ± 0.36 ↑	+0.06	1656.77 ± 0.37	1657.20 ± 0.21 ↑	+0.03
7	1541.38 ± 0.10	1542.24 ± 0.17 ↑	+0.06	1548.52 ± 0.21	1549.15 ± 0.24 ↑	+0.04	1540.75 ± 0.31	1541.25 ± 0.20 ↑	+0.03
9	1260.39 ± 0.34	1263.44 ± 0.92 ↑	+0.24	1282.57 ± 0.55	1281.84 ± 0.44 ↓	−0.06	1261.82 ± 0.28	1260.77 ± 0.33 ↓	−0.08
10	1238.61 ± 0.12	1239.03 ± 0.09 ↑	+0.03	1240.57 ± 0.54	1238.69 ± 0.07 ↓	−0.15	1238.69 ± 0.07	1238.46 ± 0.52 ↓	−0.02
12	1082.77 ± 0.15	1085.15 ± 0.79 ↑	+0.22	1080.55 ± 0.12	1079.31 ± 0.23 ↓	−0.11	1088.76 ± 1.47	1086.84 ± 0.87 ↓	−0.18

The + indicates increases and the − shows decreases in the band area and band frequency values.

The values are the mean \pm SEM for each group. Comparisons were made using Mann–Whitney U test. Downward arrow indicates a decrease and upward arrow indicates an increase in simvastatin-treated muscles with respect to that of their respective control muscles.

* $p < 0.05$.

** $p < 0.01$.

*** $p < 0.001$.

^a Represents the percent changes in each type of simvastatin-treated muscle samples with respect to control ones.

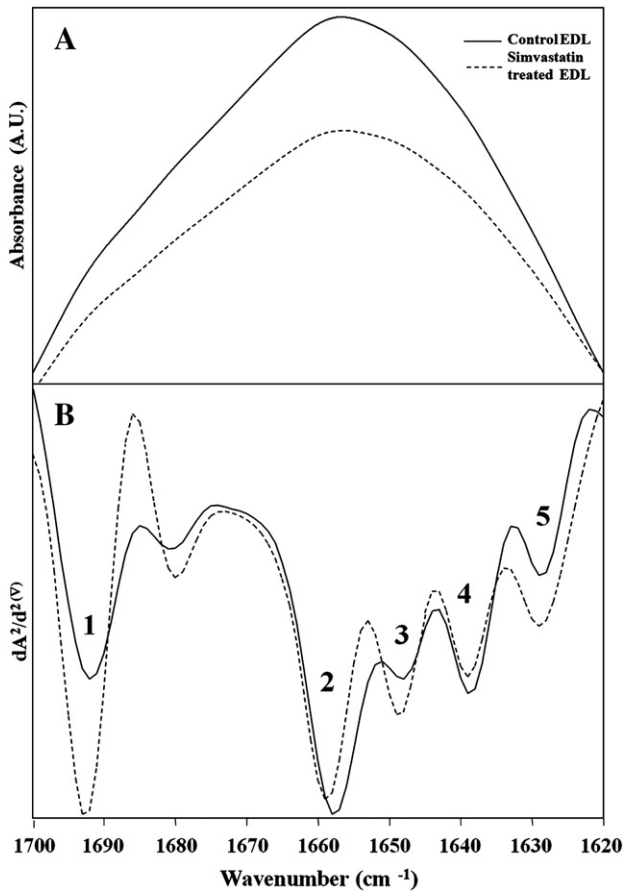


Fig. 3. Representative absorbance spectra (A) and second derivative (B) infrared spectra of control and simvastatin-treated EDL muscles in the 1700–1620 cm^{-1} region.

Changes in cholesterol esters and triglyceride contents of muscle samples were determined from area ratio of the bands located at 1741 cm^{-1} (band 5) and 1170 cm^{-1} (band 11) [11,18], which revealed a significant decrease in simvastatin-treated EDL muscles (Table 5).

The effects of simvastatin treatment on the collagen and glycogen levels of the skeletal muscles were determined from the area of the bands at 1342 cm^{-1} and 1044 cm^{-1} , respectively [15]. Simvastatin treatment reduced the collagen band area only in EDL muscle. However, glycogen band areas were significantly decreased in all simvastatin-treated muscles (Table 5).

Simvastatin-induced alterations in the nucleic acid contents of the skeletal muscles were determined from the analysis of the bands at 1261 cm^{-1} (band 9), 1236 cm^{-1} (band 10), and 1080 cm^{-1} (band 12) [11,15]. Simvastatin treatment significantly reduced the area of all three nucleic acid bands in the EDL and DIA (Table 5). However, for the SOL, simvastatin significantly reduced only the area of the nucleic acid band located at 1080 cm^{-1} .

Finally, to characterize and differentiate the simvastatin-treated and control groups based on the spectral differences in the FTIR data, hierarchical cluster analysis was performed (Fig. 4). HCA is the most popular unsupervised classification method in which “distances” between samples are calculated and displayed in a dendrogram. Dendrograms are created based on the similarities between spectra and clustering algorithms [19,20]. In dendrograms, the differences between clusters can be expressed by the heterogeneity value. A higher value indicates more spectral differences between clustered groups. It has been shown that FTIR spectroscopy together with HCA can successfully discriminate and characterize bacteria species, different diseases such as diabetes, and cancer at the cellular and tissue levels [11,19–21]. Therefore, the combination of both methods provides fast, easy, efficient, and reliable characterization of different biological systems. In our study, the dendrograms showed that all samples obtained from the controls and simvastatin-treated rats were successfully differentiated (8/8). The highest and the lowest heterogeneity values were found in EDL and SOL muscles, respectively.

4. Discussion

We evaluated the effects of chronic simvastatin treatment on the contractile and molecular structural properties of three different rat skeletal muscles to understand whether statin preferentially influences fast- or slow-twitch muscles. For this purpose, we examined the effect of simvastatin treatment on EDL muscles for fast-twitch muscle, SOL muscles for slow-twitch muscle, and DIA muscles for the mixed-twitch muscle.

In humans, the highest therapeutic dose of simvastatin is 80 mg/day [22], which corresponds to 50–100 (mg/kg)/day in animals. [16]. It has been previously shown that the metabolism of statins, especially simvastatin, in rat liver is significantly higher than in human liver, consequently yielding a lower blood concentration in rats due to the fast clearance of the drug from the blood and poor bioavailability [23–25]. Moreover, it has been shown that rats are more resistant than humans to changes in serum cholesterol [26]. Therefore, to obtain similar reduction rates in the blood cholesterol level between rats and humans, higher statin doses are required in rats. For this reason, we used a simvastatin

Table 6

Changes in the intensities of the main protein secondary structures for control and simvastatin-treated EDL, DIA, and SOL muscles.

Band no.	Band intensity								
	EDL			DIA			SOL		
	Control (n = 8)	Simvastatin (n = 8)	% change ^a	Control (n = 8)	Simvastatin (n = 8)	% change	Control (n = 8)	Simvastatin (n = 8)	% change
1	-0.13 ± 0.01	$-0.16 \pm 0.001^{***}$	+23.08	-0.023 ± 0.01	$-0.26 \pm 0.04^{\dagger}$	+13.04	-0.15 ± 0.02	$-0.16 \pm 0.01^{\dagger}$	+6.67
2	-0.20 ± 0.00	$-0.17 \pm 0.001^{***}$	–15.00	-0.12 ± 0.01	$-0.11 \pm 0.02_{\downarrow}$	–8.33	-0.1 ± 0.01	$-0.09 \pm 0.02_{\downarrow}$	–10.00
3	-0.11 ± 0.00	$-0.13 \pm 0.01^{\dagger}$	+18.18	-0.02 ± 0.01	$-0.03 \pm 0.02^{\dagger}$	+50.00	-0.09 ± 0.02	$-0.1 \pm 0.01^{\dagger}$	+11.11
4	-0.10 ± 0.00	$-0.08 \pm 0.001^{***}$	–20.00	-0.14 ± 0.01	$-0.13 \pm 0.02_{\downarrow}$	–7.14	-0.12 ± 0.01	$-0.11 \pm 0.02_{\downarrow}$	–8.33
5	-0.04 ± 0.00	$-0.06 \pm 0.01^{\dagger}$	+50.00	-0.25 ± 0.01	$-0.26 \pm 0.02^{\dagger}$	+4.00	-0.07 ± 0.01	$-0.08 \pm 0.02^{\dagger}$	+14.29

1—Antiparallel β sheet, 2— α helix, 3—random coil, 4— β sheet, and 5—aggregated β sheet.

The + indicates increases and the – shows decreases in the band area and band frequency values.

The values are the mean \pm SEM for each group. Comparisons were made using Mann–Whitney U test. Downward arrow indicates a decrease and upward arrow indicates an increase in simvastatin-treated muscles with respect to that of their respective control muscles.

* $p < 0.05$.

*** $p < 0.001$.

^a Shows the percentage changes in the each type of simvastatin-treated muscle samples with respect to control ones.

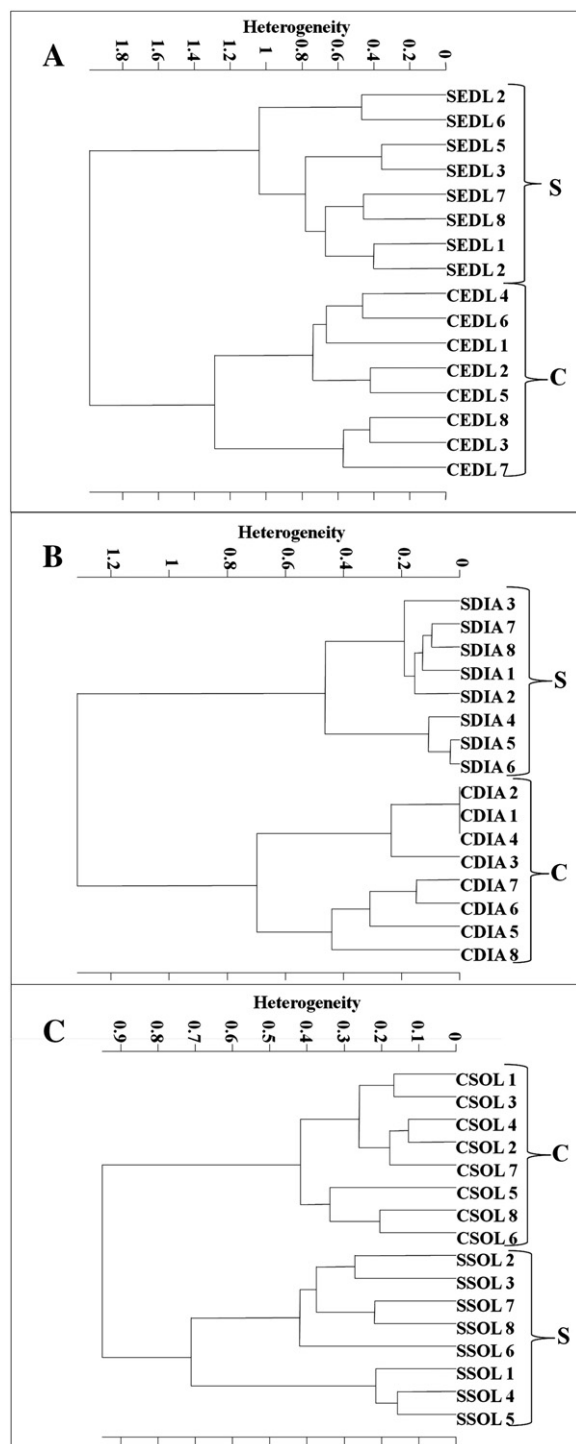


Fig. 4. Hierarchical clustering of control and simvastatin-treated (A) EDL, (B) DIA, and (C) SOL muscles. Clustering was performed using Ward's algorithm and second derivative spectra in the spectral range of 3050–1000 cm^{-1} . C: control, S: simvastatin treatment.

dose of 50 (mg/kg)/day, which is comparable to previous studies and to human doses [12,16,27,28].

The rise in total serum CK activity and myoglobin content after simvastatin treatment was indicative of the drug-induced myotoxicity in these muscles. Simvastatin treatment decreased contractile force output in all muscles but more significantly in the DIA and EDL. Simvastatin treatment also caused alterations in the macromolecular contents, lipid order, and membrane fluidity of all muscle types. These changes were more substantial in the EDL muscles.

Our experiments revealed that chronic simvastatin treatment depressed the force–frequency curves in a muscle-fiber-type-dependent manner. The extent of the simvastatin-induced contractile depression was more prominent in the EDL and DIA than the SOL. Contractile dysfunction was not related to muscle atrophy since the muscle weights were not significantly different after simvastatin treatment, although a small decrease in the body weight of simvastatin-treated rats was observed. It is commonly known that any changes in body weight affect the body fat content first since body weight changes are strongly related to the energy expenditure and body fat is the primary energy store in body [29]. Therefore, the small decrease in body weight we observed may be related to a decrease in body fat content and not to a decrease in muscle mass content. Moreover, it has been shown that skeletal muscle weight or mass is determined from the net result of the balance between protein synthesis and protein degradation. These processes are mainly coordinated by a web of intricate signaling networks, such as AKT1/FOXOs/Atrogin-1(MAFbx)/MuRF1, and the atrogin-1 gene is thought to have a role in development of statin-induced muscle atrophy [30]. Moreover, increased atrogin-1 expression leads to the loss of muscle weight [31]. In a previous study, increased atrogin-1 expression was found in statin-treated muscles, but no increase in atrogin-1 expression in human muscle biopsies after statin treatment has also been reported [32,33]. Thus, whether or not statins affect muscle weight is still unclear. Similar to our results, Westwood et al. [12] also did not observe any skeletal muscle loss after chronic simvastatin administration up to 60 (mg/kg)/day in rats.

To investigate the mechanism of this contractile impairment, we evaluated the possible contribution of impaired Ca^{2+} handling in muscle cells by studying caffeine-induced contractions. High concentrations of caffeine are known to mobilize Ca^{2+} stores by activating ryanodine receptors [34]. Therefore, the reduced responses induced by caffeine can be explained by the reduction of sarcoplasmic reticulum (SR) Ca^{2+} content, ryanodine receptor activity, or impairment of the contractile machinery beyond the release of Ca^{2+} from the SR. Time courses of caffeine-induced contractions obtained from the EDL and DIA did not differ between the controls and the simvastatin-treated muscles. These findings show that intracellular Ca^{2+} handling and/or ryanodine receptor activity were not appreciably impaired since modification of Ca^{2+} stores or ryanodine receptors is accompanied by time course alterations [35]. Thus, the reduced amplitudes of the caffeine-induced contractions in the EDL and DIA muscles can be explained by a decreased efficiency of the contractile machinery. The insignificant reduction in the amplitudes of caffeine-induced contractions in the SOL muscles supports our contractility findings, suggesting that SOL muscles are less affected. Similarly, Westwood et al. [12] reported that slow-type fibers are affected to a lesser extent by statin treatment.

We used FTIR spectroscopy to further evaluate the simvastatin-induced contractility impairment in EDL, DIA and SOL muscles at the molecular level. The band area calculations in the FTIR study revealed that simvastatin treatment decreased the glycogen, lipid, nucleic acid, protein, and collagen contents of the skeletal muscles. These alterations were found to be more pronounced in the EDL muscles than the other two muscle types.

The observed decrease in protein content in the skeletal muscles after simvastatin treatment may be due to an increase in protein degradation. In a drug-altered state, muscle cells may use proteins as an alternative energy source, eventually leading to increased protein degradation. It has been suggested that extreme protein degradation damages the muscle if the condition prevails for a long period of time [36]. Moreover, Urso et al. [32] indicated that, with exercise, statins induce variations in the gene expressions involved in the ubiquitin proteasome pathway (UPP), which is responsible for recognizing and degrading many skeletal muscle proteins and supports the observed increase in protein degradation.

The reduction in protein induced by statins may also result from a decrease in protein synthesis. Camerino et al. recently investigated statin-induced alterations in the proteomic profile of EDL muscle [37].

In that study, it was found that simvastatin treatment leads to the downregulation in the expression of proteins such as myofibrillar proteins and the proteins involved in energy production and detoxification systems [37]. The decrease in the synthesis of myofibrillar proteins such as actin, myosin, and troponin can lead to the impairment of contractile function, which supports our results on the deficiency of muscle contractility [38]. In addition to the decreased protein content, we observed a reduction in the phosphate stretching band content, implying a decrease in the relative nucleic acid content. These findings also imply that the diminished protein synthesis possibly contributes to the decreased protein levels. Although our analysis cannot differentiate between mitochondrial and cellular nucleic acid levels, it has been shown that simvastatin lowers both cellular and mitochondrial DNA contents [39]. A reduction in the mitochondrial nucleic acid content will also contribute to the impairment of oxidative energy metabolism by inhibiting mitochondrial enzyme synthesis. In addition to decreased levels of muscle proteins, we also observed a conformational change in the muscle proteins, observed by the reduction of the bandwidth and a shift in the frequency of amide I band [40]. Further analysis of this conformational change revealed an increase in random coil and aggregated β -sheet structures, which suggests protein denaturation [11,15]. The cumulative effect of all these structural changes may be the major factor leading to the impairment of skeletal muscle contractility.

In support of our results showing a decrease in lipid content (saturated and unsaturated lipids, triglyceride, and cholesterol ester), Yamazaki et al. reported a reduction in the total cholesterol content of the skeletal muscles [41]. This reduction of the muscle lipid content may be explained by an increase in lipolysis, overutilization of cellular lipid sources, or an inadequate lipid supply from the bloodstream. Since the skeletal muscles derive lipids mainly from the lipoproteins in the blood, a decrease in blood lipids may partially explain why lipids are reduced by simvastatin in the skeletal muscles. Statin treatment also impairs the β -oxidation of lipids, leading to further compromised energy metabolism and a shift to other energy sources such as carbohydrates and proteins [4].

Simvastatin treatment was reported to decrease the synthesis of coenzyme Q/ubiquinone: a powerful antioxidant and membrane stabilizer that is used in mitochondria for electron transport [41]. Decreased levels of ubiquinone lead to a further disruption in mitochondrial energy production due to increased peroxidation of the mitochondrial membrane lipids [42]. Additionally, the increase in lipid peroxidation also affects the cellular membrane and may lead to a decrease in unsaturated acyl chains, implicated by the decreased area of the olefinic band observed in our study [43].

In simvastatin-treated muscles, an observed increase in membrane rigidity (increased lipid order) and fluidity were identified based on a shift in the peak frequency to lower values and an increase in the bandwidth of the CH_2 asymmetric stretching vibration, respectively [39]. Generally, an increase in lipid order is accompanied by a decrease in membrane fluidity. However, we obtained opposite results to this general behavior, implying domain formation in membranes, which has different physical properties. This type of behavior has been previously reported for other drugs [44,45]. Indeed, we recently observed simvastatin-induced lateral phase separation (domain formation) in model membranes using a differential scanning calorimetry technique [46], which also supports our results related to the membrane fluidity and lipid order in the skeletal muscles.

The amounts of proteins and lipids and their ratios in membranes are important factors affecting membrane structure and dynamics [47]. It has been shown that the variations in the lipid-to-protein ratio and the saturated-to-unsaturated lipid ratio alter membrane thickness and curvature and thus affect membrane order, fluidity, and ion channel kinetics [48]. In our study, the increase in lipid order and membrane fluidity in the membranes induced by simvastatin results from changes in the lipid and protein contents and their ratio. Moreover, the increase in lipid order may be also due to an increase in drug-induced free radical

concentrations since free radicals modify the lipid composition of the membranes [49]. Increased membrane fluidity seems to originate from the simvastatin-induced reduction of membrane cholesterol content because it is linearly correlated with fluidity in liquid crystalline phase of the membrane [42].

Lipid order (lipid acyl chain flexibility) is a structural parameter and directly related to membrane thickness. Lipid dynamics are a functional parameter related to membrane fluidity and permeability. These parameters have an important role in regulating many membrane functions, such as signal transduction, solute transport, and activity of enzymes associated with the membrane. Recent studies provide evidence that membrane fluidity and lipid order affect ion channel kinetics and function [48]. Sirvent et al. recently reported that a change in membrane fluidity induced by statins influences the function of different ionic channels, including sodium, potassium, and chloride, and thus alters the membrane excitability [50]. Moreover, statin-induced changes in chloride conductance and the mechanical threshold of rat skeletal muscles have been shown in several studies [51,52], and it has been shown that sodium, potassium, and chloride channels have an important role in the excitation–contraction coupling of the skeletal muscle. Therefore, we conclude that statin-induced alterations in membrane fluidity and lipid order modify the function of these channels and thus contribute to the statin-induced impairment of skeletal muscle contraction–relaxation.

Membrane proteins display sensitivity to the order and fluidity of the lipid environment [53]. The function of membrane proteins may be affected by electrostatic factors and specific lipid–protein interactions depending on steric factors such as the lengths and structures of the acyl chains and the head group size of the lipids [54,55]. Changes in the phospholipid composition may also alter the secondary, tertiary, and quaternary structures of membrane proteins [56]. Although FTIR spectroscopy cannot distinguish specific proteins, in the present study, it revealed that simvastatin changes the secondary structure of some proteins by decreasing α -helix and β -sheet content and increasing aggregated β -sheet and random coil structures, implying protein denaturation.

In this study, simvastatin differentially altered the molecular structure and function of the skeletal muscles according to fast- or slow-twitch content, with the SOL being the least and the EDL being the most affected. The higher and lower heterogeneity values for the EDL and SOL muscles obtained from cluster analysis imply more and fewer differences in the spectra from the control and simvastatin-treated EDL and SOL muscles, respectively. This result supports the hypothesis that statin-induced myotoxicity is predominantly observed in EDL muscles. The resistance of the soleus or the sensitivity of the EDL muscles to statins can be related to the differences in their fiber-type content since different fiber types have different mitochondrial contents and energetics [57]. It has been known that type-II fiber-rich EDL muscles are fast-twitch glycolytic muscles with low mitochondria content, whereas type-I fiber-rich SOL muscles are slow-twitch oxidative muscles with a high mitochondria content [58]. Moreover, it has been suggested that the impairment of energy metabolism and energy depletion due to mitochondrial dysfunction in muscle tissue is the first process in statin-induced myotoxicity [59]. Recent studies reported that simvastatin treatments increase mitochondrial sensitivity to the complex-I-linked substrate (glutamate) in the skeletal muscle [60]. Moreover, the complex I substrate has been preferentially used by mitochondria in type-II fiber-rich muscles [61]. Therefore, we can infer that EDL muscle is primarily and mostly affected by statins as a result of low mitochondria content since statin-induced mitochondrial deficiency leads to an energy impairment in muscle. However, SOL muscle is not affected since it has higher mitochondria content. The resistance of this muscle type to drug treatment can also be explained by the increase PPAR γ coactivator 1 α (PGC-1 α) activity in oxidative muscle fibers, which has a role in mitochondrial biogenesis and oxidative metabolism [62].

In our previous study, we investigated the statin-induced macromolecular alterations of low-dose simvastatin treatment (20 mg/kg) in EDL muscle [11]. Similar to our spectral results, such as a decrease in protein, lipid, and nucleic acid content and an increase in membrane order and lipid fluidity, were obtained for the EDL. However, there were fewer changes in the spectral parameters for the EDL in the low-dose drug application compared to the current study [11]. In a histopathological study supporting our findings, Westwood et al. [12] showed that high doses (80 mg/kg) of statins led to skeletal muscle necrosis and that the muscles with a substantial proportion of type-IIb fast-twitch fibers (EDL) were more severely affected. In that study, it was also shown that the severe drug-induced muscle necrosis occurred in EDL muscle by the 12th day of drug administration. Moreover, it was reported that the administration of 20 mg/kg simvastatin for 8 weeks led to necrosis-related symptoms, such as infiltrates, round, angular, polymorphic fibers, the process of phagocytosis, and loss of the sarcolemma, in drug-treated rat gastrocnemius muscle [59]. Profound necrosis in rabbit EDL muscle was also observed by Nakahara et al. after administering 50 mg/kg simvastatin for 4 weeks [63], which is a similar dose and duration of simvastatin treatment to that used in our study. However, we used rats in our study, not rabbits, so this species difference could explain why rat muscles were not as severely affected by simvastatin treatment as rabbit muscles. Although we did not evaluate simvastatin-induced necrosis in muscles histopathologically, the muscle necrosis in EDL muscle can also be deduced from our contractile and spectral results. For example, the degeneration of myofibers has been shown in simvastatin-treated EDL muscles [12], which could be related to the degradation of contractile proteins. Therefore, the decrease in the protein content of simvastatin-treated muscles we observed is indicative of muscle necrosis.

In conclusion, chronic simvastatin treatment in rats significantly inhibited the force output of the skeletal muscles, and this impairment was more severe in fast-twitch muscles than in slow-twitch muscles. In parallel with our contractility results, the spectral results also showed that fast-type muscles were preferentially injured. These structural alterations are regarded as the molecular basis of statin-induced skeletal muscle toxicity.

Funding information

This work was supported by Middle East Technical University and State Planning Organization (METU-DPT Research Fund, Grant Number BAP-08-11-DPT2002K120510-TB-04).

Acknowledgement

We would like to thank Dr. Okkes Yilmaz for the HPLC serum cholesterol measurements.

References

- [1] M. Evans, A. Rees, Effects of HMG-CoA reductase inhibitors on skeletal muscle — are all statins the same? *Drug Saf.* 25 (2002) 649–663.
- [2] M. Fukami, N. Maeda, J. Fukushima, Y. Kogure, Y. Shimada, T. Ogawa, Y. Tsujita, Effects of HMG-CoA reductase inhibitors on skeletal muscles of rabbits, *Res. Exp. Med. (Berl)* 193 (1993) 263–273.
- [3] S. Guis, D. Figarella-Branger, J.P. Mattei, F. Nicoli, Y. Le Fur, G. Kozak-Ribbens, J.F. Pellissier, P.J. Cozzone, N. Amabile, D. Bendahan, In vivo and in vitro characterization of skeletal muscle metabolism in patients with statin-induced adverse effects, *Arthritis Rheum.* 55 (2006) 551–557.
- [4] P. Kaufmann, M. Torok, A. Zahno, K.M. Waldhauser, K. Brecht, S. Krahenbuhl, Toxicity of statins on rat skeletal muscle mitochondria, *Cell. Mol. Life Sci.* 63 (2006) 2415–2425.
- [5] B.A. Hamelin, J. Turgeon, Hydrophilicity/lipophilicity: relevance for the pharmacology and clinical effects of HMG-CoA reductase inhibitors, *Trends Pharmacol. Sci.* 19 (1998) 26–37.
- [6] Y. Levy, R. Leibowitz, M. Aviram, J.G. Brook, U. Cogan, Reduction of plasma cholesterol by lovastatin normalizes erythrocyte membrane fluidity in patients with severe hypercholesterolemia, *Br. J. Clin. Pharmacol.* 34 (1992) 427–430.
- [7] I. Morita, I. Sato, L. Ma, S. Murota, Enhancement of membrane fluidity in cholesterol-poor endothelial cells pre-treated with simvastatin, *Endothelium* 5 (1997) 107–113.
- [8] S. Pierno, A. De Luca, D. Tricarico, A. Roselli, F. Natuzzi, E. Ferrannini, M. Laico, D.C. Camerino, Potential risk of myopathy by HMG-CoA reductase inhibitors: a comparison of pravastatin and simvastatin effects on membrane electrical properties of rat skeletal muscle fibers, *J. Pharmacol. Exp. Ther.* 275 (1995) 1490–1496.
- [9] E.G. Bliznakov, D.J. Wilkins, Biochemical and clinical consequences of inhibiting coenzyme Q(10) biosynthesis by lipid-lowering HMG-CoA reductase inhibitors (statins): a critical overview, *Adv. Ther.* 15 (1998) 218–228.
- [10] C. Guijarro, L.M. Blanco-Colio, M. Ortego, C. Alonso, A. Ortiz, J.J. Plaza, C. Diaz, G. Hernandez, J. Egido, 3-Hydroxy-3-methylglutaryl coenzyme A reductase and isoprenylation inhibitors induce apoptosis of vascular smooth muscle cells in culture, *Circ. Res.* 83 (1998) 490–500.
- [11] N.S. Ozek, Y. Sara, R. Onur, F. Severcan, Low dose simvastatin induces compositional, structural and dynamic changes in rat skeletal extensor digitorum longus muscle tissue, *Biosci. Rep.* 30 (2010) 41–50.
- [12] F.R. Westwood, A. Bigley, K. Randall, A.M. Marsden, R.C. Scott, Statin-induced muscle necrosis in the rat: distribution, development, and fibre selectivity, *Toxicol. Pathol.* 33 (2005) 246–257.
- [13] H. Obayashi, Y. Nezu, H. Yokota, N. Kiyosawa, K. Mori, N. Maeda, Y. Tani, S. Manabe, A. Sanbuihso, Cerivastatin induces type-I fiber-, not type-II fiber-, predominant muscular toxicity in the young male F344 rats, *J. Toxicol. Sci.* 36 (2011) 445–452.
- [14] F. Severcan, P. Haris, Vibrational Spectroscopy in Diagnosis and Screening, First edition IOS Press, UK, 2012.
- [15] G. Cakmak, F. Zorlu, M. Severcan, F. Severcan, Screening of protective effect of amifostine on radiation-induced structural and functional variations in rat liver microsomal membranes by FT-IR spectroscopy, *Anal. Chem.* 83 (2011) 2438–2444.
- [16] L.N. Johnson-Anuna, G.P. Eckert, J.H. Keller, U. Igbavboa, C. Franke, T. Fechner, M. Schubert-Zsilavecz, M. Karas, W.E. Muller, W.G. Wood, Chronic administration of statins alters multiple gene expression patterns in mouse cerebral cortex, *J. Pharmacol. Exp. Ther.* 312 (2005) 786–793.
- [17] Ö. Yilmaz, S. Keser, M. Tuzcu, B. Çetintas, Resveratrol (trans-3,4',5-trihydroxystilbene) decreases lipid peroxidation level and protects antioxidant capacity in sera and erythrocytes of old female Wistar rats induced by the kidney carcinogen potassium bromate, *Environ. Toxicol. Pharmacol.* 24 (2007) 79–85.
- [18] M. Nara, M. Okazaki, H. Kagi, Infrared study of human serum very-low-density and low-density lipoproteins. Implication of esterified lipid C=O stretching bands for characterizing lipoproteins, *Chem. Phys. Lipids* 117 (2002) 1–6.
- [19] P. Lasch, W. Haensch, D. Naumann, M. Diem, Imaging of colorectal adenocarcinoma using FT-IR microspectroscopy and cluster analysis, *Biochim. Biophys. Acta* 1688 (2004) 176–186.
- [20] F. Severcan, O. Bozkurt, R. Gurbanov, G. Gorgulu, FT-IR spectroscopy in diagnosis of diabetes in rat animal model, *J. Biophotonics* 3 (2010) 621–631.
- [21] F. Draux, P. Jeannesson, C. Gobinet, J. Sule-Suso, J. Pijanka, C. Sandt, P. Dumas, M. Manfait, G.D. Sockalingum, IR spectroscopy reveals effect of non-cytotoxic doses of anti-tumour drug on cancer cells, *Anal. Bioanal. Chem.* 395 (2009) 293–301.
- [22] T.N. Patel, M.H. Shishehbor, D.L. Bhatt, A review of high-dose statin therapy: targeting cholesterol and inflammation in atherosclerosis, *Eur. Heart J.* 28 (2007) 664–672.
- [23] T. Prueksaritanont, R. Subramanian, X. Fang, B. Ma, Y. Lin, J.H. Qiu, P.G. Pearson, T.A. Baillie, Glucuronidation of statins in animals and humans: a novel mechanism of statin lactonization, *Drug Metab. Dispos.* 30 (2002) 505–512.
- [24] M. Boberg, R. Angerbauer, W.K. Kanhai, W. Karl, A. Kern, M. Radtke, W. Steinke, Biotransformation of cerivastatin in mice, rats, and dogs in vivo, *Drug Metab. Dispos.* 26 (1998) 640–652.
- [25] T. Komai, K. Kawai, T. Tokui, Y. Tokui, C. Kuroiwa, E. Shigehara, M. Tanaka, Disposition and metabolism of pravastatin sodium in rats, dogs and monkeys, *Eur. J. Drug Metab. Pharmacokinet.* 17 (1992) 103–113.
- [26] W.E. Stehbens, An appraisal of cholesterol feeding in experimental atherogenesis, *Prog. Cardiovasc. Dis.* 29 (1986) 107–128.
- [27] N. Cartier, S. Guidoux, F. Rocchiccioli, P. Aubourg, Simvastatin does not normalize very long chain fatty acids in adrenoleukodystrophy mice, *FEBS Lett.* 478 (2000) 205–208.
- [28] S. Youssef, O. Stuve, J.C. Patarroyo, P.J. Ruiz, J.L. Radosevich, E.M. Hur, M. Bravo, D.J. Mitchell, R.A. Sobel, L. Steinman, S.S. Zamvil, The HMG-CoA reductase inhibitor, atorvastatin, promotes a Th2 bias and reverses paralysis in central nervous system autoimmune disease, *Nature* 420 (2002) 78–84.
- [29] R.E. Keesey, T.L. Powley, The regulation of body weight, *Annu. Rev. Psychol.* 37 (1986) 109–133.
- [30] G.A. Nader, Molecular determinants of skeletal muscle mass: getting the “AKT” together, *Int. J. Biochem. Cell Biol.* 37 (2005) 1985–1996.
- [31] M.D. Gomes, S.H. Lecker, R.T. Jagoe, A. Navon, A.L. Goldberg, Atrogin-1, a muscle-specific F-box protein highly expressed during muscle atrophy, *Proc. Natl. Acad. Sci. U. S. A.* 98 (2001) 14440–14445.
- [32] M.L. Urso, P.M. Clarkson, D. Hittel, E.P. Hoffman, P.D. Thompson, Changes in ubiquitin proteasome pathway gene expression in skeletal muscle with exercise and statins, *Arterioscler. Thromb. Vasc. Biol.* 25 (2005) 2560–2566.
- [33] J.L. Hanai, P. Cao, P. Tanksale, S. Imamura, E. Koshimizu, J. Zhao, S. Kishi, M. Yamashita, P.S. Phillips, V.P. Sukhatme, S.H. Lecker, The muscle-specific ubiquitin ligase atrogin-1/MAFbx mediates statin-induced muscle toxicity, *J. Clin. Invest.* 117 (2007) 3940–3951.
- [34] C. Franzini-Armstrong, F. Protasi, Ryanodine receptors of striated muscles: a complex channel capable of multiple interactions, *Physiol. Rev.* 77 (1997) 699–729.

- [35] R. Sitsapesan, A.J. Williams, Regulation of current flow through ryanodine receptors by luminal Ca^{2+} , *J. Membr. Biol.* 159 (1997) 179–185.
- [36] K. Motojima, P. Passilly, J.M. Peters, F.J. Gonzalez, N. Latruffe, Expression of putative fatty acid transporter genes are regulated by peroxisome proliferator-activated receptor alpha and gamma activators in a tissue- and inducer-specific manner, *J. Biol. Chem.* 273 (1998) 16710–16714.
- [37] G.M. Camerino, M.A. Pellegrino, L. Brocca, C. Digennaro, D.C. Camerino, S. Pierno, R. Bottinelli, Statin or fibrate chronic treatment modifies the proteomic profile of rat skeletal muscle, *Biochem. Pharmacol.* 81 (2011) 1054–1064.
- [38] V. Barone, F. Bertocchini, R. Bottinelli, F. Protasi, P.D. Allen, C. Franzini Armstrong, C. Reggiani, V. Sorrentino, Contractile impairment and structural alterations of skeletal muscles from knockout mice lacking type 1 and type 3 ryanodine receptors, *FEBS Lett.* 422 (1998) 160–164.
- [39] B.A. Schick, R. Laaksonen, J.J. Frohlich, H. Paiva, T. Lehtimäki, K.H. Humphries, H.C. Cote, Decreased skeletal muscle mitochondrial DNA in patients treated with high-dose simvastatin, *Clin. Pharmacol. Ther.* 81 (2007) 650–653.
- [40] P.I. Haris, F. Severcan, FTIR spectroscopic characterization of protein structure in aqueous and non-aqueous media, *J. Mol. Catal. B. Enzym.* 7 (1999) 207–221.
- [41] H. Yamazaki, M. Suzuki, T. Aoki, S. Morikawa, T. Maejima, F. Sato, K. Sawanobori, M. Kitahara, T. Kodama, Y. Saito, Influence of 3-hydroxy-3-methylglutaryl coenzyme A reductase inhibitors on ubiquinone levels in rat skeletal muscle and heart: relationship to cytotoxicity and inhibitory activity for cholesterol synthesis in human skeletal muscle cells, *J. Atheroscler. Thromb.* 13 (2006) 295–307.
- [42] S.K. Baker, M.A. Tarnopolsky, Statin myopathies: pathophysiologic and clinical perspectives, *Clin. Invest. Med.* 24 (2001) 258–272.
- [43] R.H. Sills, D.J. Moore, R. Mendelsohn, Erythrocyte peroxidation: quantitation by Fourier transform infrared spectroscopy, *Anal. Biochem.* 218 (1994) 118–123.
- [44] F. Severcan, I. Sahin, N. Kazanci, Melatonin strongly interacts with zwitterionic model membranes—evidence from Fourier transform infrared spectroscopy and differential scanning calorimetry, *Biochim. Biophys. Acta* 668 (2005) 215–222.
- [45] F. Severcan, S. Cannistraro, Model membrane partition ESR study in the presence of α -tocopherol by a new spin probe, *Biosci. Rep.* 9 (1989) 489–495.
- [46] M. Kocak, F. Severcan, Interactions of cholesterol reducing agent simvastatin with neutral DPPC and DMPC multilamellar liposomes, *Biophysical Society Meeting Abstracts Supplement*, *Biophys. J.*, 2007, p. 59a.
- [47] B. Szalontai, Y. Nishiyama, Z. Gombos, N. Murata, Membrane dynamics as seen by Fourier transform infrared spectroscopy in a cyanobacterium, *Synechocystis* PCC 6803. The effects of lipid unsaturation and the protein-to-lipid ratio, *Biochim. Biophys. Acta* 1509 (2000) 409–419.
- [48] M.S. Awayda, W. Shao, F. Guo, M. Zeidel, W.G. Hill, ENaC–membrane interactions: regulation of channel activity by membrane order, *J. Gen. Physiol.* 123 (2004) 709–727.
- [49] R. Kinder, C. Ziegler, J.M. Wessels, Gamma-irradiation and UV-C light-induced lipid peroxidation: a Fourier transform-infrared absorption spectroscopic study, *Int. J. Radiat. Biol.* 71 (1997) 561–571.
- [50] P. Sirvent, J. Mercier, A. Lacampagne, New insights into mechanisms of statin-associated myotoxicity, *Curr. Opin. Pharmacol.* 8 (2008) 333–338.
- [51] S. Pierno, A. De Luca, A. Liantonio, C. Camerino, D. Conte Camerino, Effects of HMG-CoA reductase inhibitors on excitation–contraction coupling of rat skeletal muscle, *Eur. J. Pharmacol.* 364 (1999) 43–48.
- [52] S. Pierno, M.P. Didonna, V. Cipponi, A. De Luca, M. Pisoni, A. Frigeri, G.P. Nicchia, M. Svelto, G. Chiesa, C. Sirtori, E. Scanziani, C. Rizzo, D. De Vito, D. Conte Camerino, Effects of chronic treatment with statins and fenofibrate on rat skeletal muscle: a biochemical, histological and electrophysiological study, *Br. J. Pharmacol.* 149 (2006) 909–919.
- [53] A.G. Lee, Lipids and their effects on membrane proteins: evidence against a role for fluidity, *Prog. Lipid Res.* 30 (1991) 323–348.
- [54] A. Carruthers, D.L. Melchior, How bilayer lipids affect membrane protein activity, *Trends Biochem. Sci.* 11 (1986) 331–335.
- [55] K. Turnheim, J. Gruber, C. Wachter, V. Ruiz-Gutierrez, Membrane phospholipid composition affects function of potassium channels from rabbit colon epithelium, *Am. J. Physiol.* 277 (1999) C83–C90.
- [56] A.M. Kleinfeld, Current views of membrane structure, *Curr. Top. Membr. Transp.* 29 (1987) 1–27.
- [57] P.S. Phillips, R.H. Haas, Statin myopathy as a metabolic muscle disease, *Expert. Rev. Cardiovasc. Ther.* 6 (2008) 971–978.
- [58] D.E. Goll, M.H. Stromer, R.M. Robson, Skeletal muscle, nervous system, temperature regulation and special senses, in: M.J. Swenson (Ed.), *Duke's Physiology of Domestic Animals*, Cornell University Press, New York, 1977, pp. 504–530.
- [59] M.R. Bonfim, J.C.S. Camargo Filho, L.C.M. Vanderlei, Padulla, M.F. Accioly, R.S.D. Souza, R. Azoubel, Muscle response to the association of statin and physical exercise in rats, *Int. J. Morphol.* 27 (2009) 1155–1161.
- [60] S. Larsen, N. Stride, M. Hey-Mogensen, C.N. Hansen, L.E. Bang, H. Bundgaard, L.B. Nielsen, J.W. Helge, F. Dela, Simvastatin effects on skeletal muscle: relation to decreased mitochondrial function and glucose intolerance, *J. Am. Coll. Cardiol.* 61 (2013) 44–53.
- [61] E. Ponsot, J. Zoll, B. N'Guessan, F. Ribera, E. Lampert, R. Richard, V. Veksler, R. Ventura-Clapier, B. Mettauer, *J. Cell. Physiol.* 203 (2005) 479–486.
- [62] J. Lin, H. Wu, P.T. Tarr, C. Zhang, Z. Wu, O. Boss, L.F. Michael, P. Puigserver, E. Isotani, E.N. Olson, B.B. Lowell, R. Bassel-Duby, B.M. Spiegelman, Transcriptional co-activator PGC-1 α drives the formation of slow-twitch muscle fibres, *Nature* 418 (2002) 797–801.
- [63] K. Nakahara, M. Kuriyama, Y. Sonoda, H. Yoshidome, H. Nakagawa, J. Fujiyama, I. Higuchi, M. Osame, Myopathy induced by HMG-CoA reductase inhibitors in rabbits: a pathological, electrophysiological, and biochemical study, *Toxicol. Appl. Pharmacol.* 152 (1998) 99–106.